ELSEVIER

Journal of Power Sources 109 (2002) 418–421

JOURNAL OF POWER SOURCES

www.elsevier.com/locate/jpowsour

# Enhanced performance of $SnO_2$ xerogel electrochemical capacitor prepared by novel crystallization process

N.L. Wu*, C.Y. Han, S.L. Kuo

*Department of Chemical Engineering, National Taiwan University, Taipei 106, Taiwan, ROC*

Received 3 January 2002; received in revised form 3 February 2002; accepted 20 February 2002

**Abstract**

The performance of both blank and $RuO_2$-impregnated $SnO_2$ (Sb-6 mol%) xerogel electrodes are enhanced significantly by improved crystallinity via a novel crystallization process, which effectively suppresses grain coarsening and hence allows the xerogel to be crystallized at high temperatures while maintaining a high surface area. The improved $SnO_2$ electrodes show maximum specific capacitances which exceed 10 F $g^{-1}$ in 1 M $KOH_{aq}$ at 200 mV $s^{-1}$ after firing at 800 °C. The enhancement becomes increasingly pronounced with increasing charge–discharge rate due to improved oxide conductivity. 

*Keywords:* Electrochemical capacitor; Crystallization; Capacitance; Tin oxide

## 1. Introduction

Due to its chemical stability and high conductivity, $SnO_2$ has been used as the electrode material in several solution electrochemical processes [1–3]. In addition, $SnO_2$ materials of high surface area can easily be synthesized, for example, via sol–gel processes [4–7]. These properties render $SnO_2$ promising electrode material for electrochemical capacitor (EC) applications. Indeed, ECs using doped $SnO_2$ xerogel as the sole electrode component, or part of a composite electrode, have been demonstrated [8–10]. It was established [9] that a Sb-doped $SnO_2$ xerogel EC using $KOH_{aq}$ electrolyte exhibits no psedocapacitance but pure double-layer capacitive behaviors that are consistent with the classical Mott–Schottky model for a semiconductor electrolyte interface [11,12]. Accordingly, in strong electrolytes, as typically encountered in ECs, the capacitance of the entire system closely approximates to the space charge capacitance on the oxide side. The latter increases with increasing carrier concentration.

For sol–gel derived $SnO_2$, which is a heavily defected semiconductor, it is anticipated that the effective carrier concentration is determined to a great extent by defect density. High-temperature crystallization helps to remove defects and hence may increase capacitance. The gain, nevertheless, could easily be offset by a loss in surface area due to grain coarsening. For instance, it has been shown that, for Sb-doped (6 mol%) $SnO_2$ xerogel powder synthesized via the conventional sol–gel process, the specific capacitance reaches a maximum value by crystallization at 500 °C and monotonically decreases at higher crystallization temperatures [9].

We have previously demonstrated [13,14] that grain growth upon firing of hydrous powders of sol–gel derived metal oxides can be effectively suppressed by a novel crystallization process in which the surface hydroxyl groups of the oxide are replaced with siloxyl ones prior to the firing process. This process hence allows the amorphous oxide powder to be crystallized at high temperatures while maintaining a high surface area. As shown here, when it is applied to the synthesis of $SnO_2$ xerogel powder for EC applications, the capacitances of both the $SnO_2$ and $RuO_2$–$SnO_2$ composite ECs can be significantly improved. The enhancement is particularly pronounced at high charge–discharge rates and is attributed to the combination of a higher carrier concentration and an improved conductivity.

## 2. Experimental

Amorphous Sb-doped $SnO_2$ hydrous power was prepared via a two-step sol–gel process [9]. In brief, ammonia was introduced into an aqueous solution containing 0.1 M $SnC_4$ to cause the first condensation. The gelatinous precipitate

* Corresponding author. Tel.: +886-2-2363-5230; fax: +886-2-2362-3040.
*E-mail address:* nlw001@ccms.ntu.edu.tw (N.L. Wu).

0378-7753/02/$ – see front matter 
PII: S0378-7753(02)00095-2

was washed and then peptized at pH ~ 10.0. An alcoholic solution of $SbCl_3$ that gives a final Sb:Sn molar ratio of 0.06:1 was then added and this resulted in the second condensation. The second precipitate was then washed, primarily for removing $Cl^-$ and dried at 30 °C under 75% humidity. The surface pretreatment prior to firing was carried out by reacting the hydrous power with hexamethyldisilazane (HMDS; $(Si(CH_3)_3)_2NH$)) at 150 °C for 1 h. Crystallization firing was carried out in flowing air with a heating rate of 100 °C $h^{-1}$ and a holding time at selected temperatures for 1 h.

In preparing $RuO_2$–$SnO_2$ composite powder, ruthenium oxide was loaded by an incipient-wetness method, in which an aqueous solution of $RuCl_3$ was added to the crystallized $SnO_2$ xerogel powder in an amount that is just sufficient to wet completely the powder. The wetted powder was finally calcined at 200 °C in air for 5 h. The loading is within 1.2–1.4 wt.% of $RuO_2$.

For powder characterization, nitrogen adsorption (ASAP2000, Micromeritics) was conducted to determine the BET surface area, while X-ray diffraction (XRD) was performed on a Mac-Science/MXP diffractometer with Cu Kα radiation. UV absorption spectra were taken on a Hitachi U3410 spectrometer, which was equipped with an integrating sphere and deuterium and tungsten iodide lamps as light sources.

Cyclic voltammetry (CV) analysis was performed using an electrochemical analyzer (Eco Chemie PGSTAT3O) and a plane-type capacitor cell, which comprised two planar electrodes each of which had a 1 cm × 1 cm active area, a glass-fiber separator and aqueous electrolyte. The electrodes each had a thickness of approximately ~55 μm and comprised calcined powders and 3 wt.% PVDF binder which were spread on to a Ti foil. The specific capacitance for each of the electrode pairs, $C_e$ was determined by the equation, $C_e = 2[(i_c + i_a)/2]s/W$, where $i_c$ and $i_a$ are the absolute currents at 0.0 V during the cathodic and anodic sweeps, respectively, $s$ the sweep rate and $W$ the weight of the oxide in each electrode. The multiplication of two accounts for the fact that each of the electrodes forms one capacitor at the interface and hence there are two serial capacitors in one cell.

## 3. Results and discussion

The microstructural properties between the powders that have been crystallized with or without the employment of HMDS pretreatment are listed in Table 1. For simplicity, a prefix 'H' will hereafter be given to powders which have been pretreated with HMDS and 'U' to those have not. The coarsening-inhibition effect due to HMDS treatment is clear. The H-powder fired at 500 °C has a surface area of 133 $m^2\ g^{-1}$ which is twice that of the U-powder. Notably, the H-powder fired at 800 °C retains a surface area (75 $m^2\ g^{-1}$) and a grain size (~4.0 nm) that are similar to those for U-powder fired at 500 °C. The inhibition effect has been attributed to the formation of Si-containing secondary-phase particles along the grain boundaries, which retard the motion of grain boundaries involved in a sintering process [3].

Table 1
Microstructural properties of Sb-doped $SnO_2$ electrodes

| | | Crystallization temperature (°C) | | | |
|---|---|---|---|---|---|
| | | 500 | 600 | 700 | 800 |
| H-powder[a] | Surface area ($m^2/g$)[b] | 133 | 102 | 103 | 75 |
| | Crystallite size (nm)[c] | 3.2 | 3.3 | 3.6 | 4.2 |
| U-powder[a] | Surface area ($m^2/g$)[b] | 66 | 38 | 30 | 25 |
| | Crystallite size (nm)[c] | 5.8 | 9.4 | 11.3 | 14.4 |

[a] H-powders refer to xerogels pretreated with HMDS prior to calcination, while U-powders are untreated.
[b] Surface area refers to BET surface area measured by $N_2$ adsorption.
[c] Crystallite size is determined by XRD analysis using Debye–Scherrer equation and full-width at half-maximum of $SnO_2$ (1 1 0) Bragg peak.

For H-powder electrodes in 1 M $KOH_{aq}$ electrolyte at a sweep rate of 20 mV $s^{-1}$ the capacitance is negligible for the 500 °C-powder (curve 1, Fig. 1), despite its very high surface area. A capacitor-like voltammogram was obtained only after firing at temperatures above 700 °C (curve 3). The capacitance reaches a maximum value of ~10.5 F $g^{-1}$ $SnO_2$ when firing at 800 °C (curve 4). This is three time the maximum capacitance achieved for the U-powder (500 °C; curve 5) at the same sweep rate. Calcination of H-powders at temperatures above 800 °C (not shown) only cause a decline in capacitance.

The effect of sweep rate on the capacitances of the two optimum powders, namely the 500 °C U- and 800 °C H-powders, is shown in Fig. 2. The blank U-powder (curve 1, Fig. 2) exhibits a sharp drop, by over 30%, in capacitance as the sweep rate increases from 4 to 20 mV $s^{-1}$. For the H-powder (curve 2), on the other hand, the capacitance remained rather rather constant at the ~10 F $g^{-1}$ level as

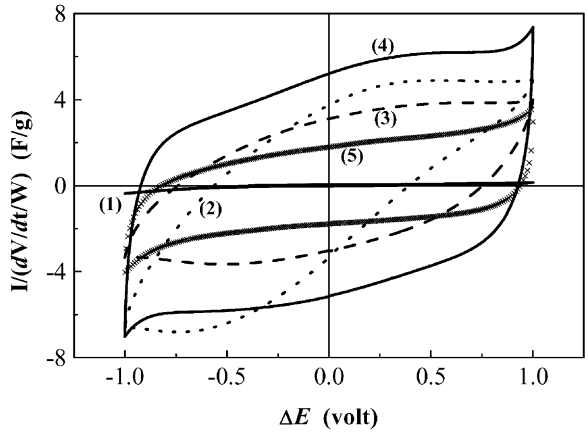


Fig. 1. Voltammograms for $SnO_2$ electrodes made of H-powders fired at: (1) 500; (2) 600; (3) 700; (4) 800 °C. (5) U-powder fired at 500 °C (electrolyte: 1 M $KOH_{aq}$; sweep rate = 20 mV $s^{-1}$).

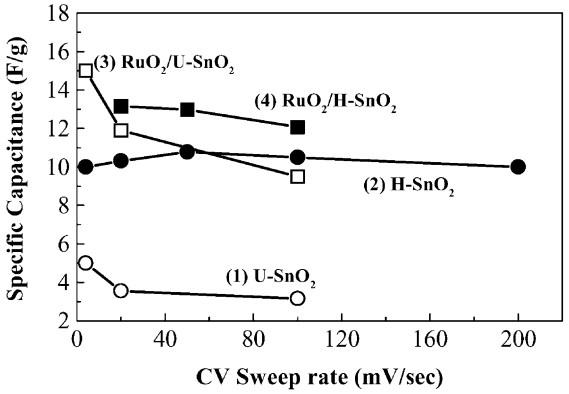


Fig. 2. Effect of CV sweep rate on specific capacitance of (1) blank U-powder, (2) blank H-powder, (3) $RuO_2$-impregiiated U-powder and (4) $RuO_2$-irnpregnated H-powder.

the sweep rates is varied by a factor of 50, i.e. from 4 to 200 mV $s^{-1}$. Clearly, the improvement due to HMDS treatment is increasingly pronounced with increasing charge–discharge rate. At 200 mV $s^{-1}$ a H-powder cell delivers a maximum power of 1 W $g^{-1}$ of total $SnO_2$ oxide.

An enhanced high-rate performance is also seen for the $RuO_2$–$SnO_2$ composite EC. In previous work [10], ruthenium oxide in nanocrystallite form was dispersed on to the $SnO_2$ xerogel electrodes to form a composite EC, in order to maximize the utilization of the well-known pseudocapacitive properties of $RuO_2$ [10]. Nevertheless, it was found that the capacitance of the composite electrodes shows approximately the same decline in capacitance with charge–discharge rate as the blank $SnO_2$ electrodes (curves 1 and 3, Fig. 2), which suggests a rate-liming mechanism associated mainly with the $SnO_2$ substrate. The high-rate performance of the composite electrodes is hence also greatly improved, as shown in Figs. 2 and 3, when the HMDS-treated $SnO_2$ xerogel powder is used as the substrate.

As pointed out earlier, there are two factors which have the most predominant effect on the specific capacitance of the Sb-doped $SnO_2$ xerogel powder, namely the specific surface area and the crystallinity. The surface area decreases, while the crystallinity increases, with increasing crystallization temperature. The competing effects of these two factors explain the existence of the maximum capacitance which occurs after firing at 500 °C for the blank U-powder [9]. Transmission electron microscopy has confirmed [4] that the sol–gel derived $SnO_2$ grains crystallized fully at this temperature. While a similar situation may be expected for the H-powder, it is further complicated by the presence of the superficial Si-containing species which result from HMDS and could deteriorate connection between the $SnO_2$ grains. A temperature higher than 500 °C may be required to optimize the microstructure at the grain boundaries in order to achieve the maximum capacitance. This may be the reason why a higher optimum crystallization temperature (800 °C) is needed for achieving maximum capacitance from the H-powder.

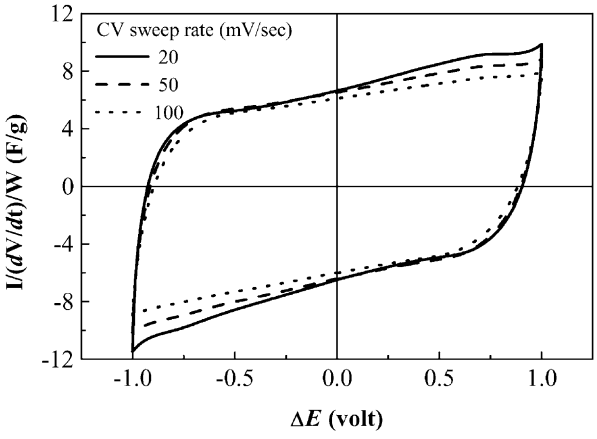


Fig. 3. Voltammograms of $RuO_2$ (1.2 wt.%)–$SnO_2$ composite xerogel electrode for which the $SnO_2$ powder is crystallized at 800 °C.

While the two optimum powders (500 °C-U and 800 °C-H powders) have approximately the same specific surface area and grain size (Table 1), the H-powder exhibits much higher capacitance (Figs. 2 and 3). The capacitance enhancement may be attributed to the presence of less intragrain defects in the H-powder due to the higher calcination temperature that is employed. This is further confirmed by a UV spectroscopy study, as shown in Fig. 4. The absorption edge energies are determined by fitting the data to the equation $(\sigma h\omega)^2 = A(h\omega - E_g)$, where $\sigma$ is the absorption coefficient, $h\omega$ the photon energy and $E_g$ the edge energy [15]. For comparison, He et al. [16] reported a bandgap of 3.83 eV for highly crystallized Sb-doped $SnO_2$ thin films. All of the test-powders, including 500, 800 °C U-powders and 800 °C H-powder show a red-shift in UV absorption with respect to the reported bandgap value. The red-shift indicates spreading in the energy of localized states introduced by defects near band edges. The extent of the spreading and hence the extent of the shift, decreases with decreasing defect density [5]. As shown in Fig. 4, the 800 °C H-powder

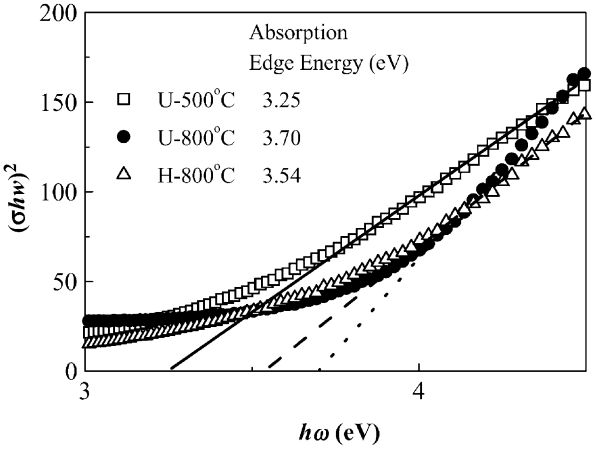


Fig. 4. UV absorption analysis. Lines fit linear portion of data according to $(\sigma h\omega)^2 = A(h\omega - E_g)$), where $\sigma$ is absorption coefficient, $h\omega$ the photon energy, $E_g$ the edge energy.

has a higher absorption edge energy and hence less defects than the 500 °C U-powder. As defect density decreases, the effective carrier concentration increases and so does the space-charge capacitance [11,12]. This is consistent with the fact that the 800 °C H-powder exhibits a larger capacitance (Fig. 1). The 800 °C U-powder, which has the highest absorption edge energy, is expected to possess the largest capacitance per unit surface area. It, nevertheless, has a specific surface area that is only one-half of those of the other two powders.

The conductivity of the oxide would also increase as the defect density decreases due to increased effective carrier concentration and carrier mobility. This factor is believed to play an important role in the enhancement of the high-rate performance for the 800 °C H-powder (Fig. 2). In addition, a slight increase in capacitance of the H-powder occurs between 4 and 50 mV $s^{-1}$ as seen in Fig. 2. This unusual behaviour may be caused by the presence of an ionic impurity, the origin of which has yet to be identified. A similar phenomenon was not, however, seen for the $RuO_2$-impregnated electrodes.

In summary, the electrochemical capacitance of both blank and $RuO_2$-impregnated Sb-doped $SnO_2$ xerogel electrode has been enhanced significantly by adopting a novel crystallization process which suppresses coarsening of the xerogel grains upon firing. The process allows the xerogel to be fired at higher temperatures while maintaining a high surface area. The capacitance enhancement, which is increasingly pronounced with increasing charge–discharge rate, has been attributed to an increase in carrier concentration as well as in oxide conductivity, both of which result from higher crystallization temperatures.

## Acknowledgements

This work is supported by the National Science Council of the Republic of China under Contract No. NSC 90-2214-E-002-009.

## References

[1] B. Correa-Lozano, Ch. Comninellis, A. De Battisti, J. Appl. Electrochem. 26 (1996) 683.
[2] B. Correa-Lozano, Ch. Comninellis, A. De Battisti, J. Appl. Electrochem. 27 (1997) 970.
[3] L. Lipp, D. Pletcher, Electrochim. Acta 42 (1997) 1091.
[4] N.L. Wu, L. Wu, Y.C. Yang, S.J. Huang, J. Mater. Res. 11 (1996) 813.
[5] N.L. Wu, L.F. Wu, I.A. Rusakova, A. Hained, A.P. Litvinchuk, J. Am. Ceram. Soc. 82 (1999) 67.
[6] S.-Y. Wang, N.-L. Wu, J. Non-Cryst. Solids 224 (1998) 259.
[7] N.-L. Wu, S.-Y. Wang, J. Mater. Sci. 34 (1999) 2807.
[8] Japan Patent No. 1-227-418.
[9] N.L. Wu, J.Y. Hwang, P.Y. Lin, C.Y. Han, S.L. Kuo, K.H. Liao, M.H. Lee, S.Y. Wang, J. Electrochem. Soc. 148 (2001) 550.
[10] N.L. Wu, S.L. Kuo, M.H. Lee, J. Power Sources 104 (2002) 62.
[11] S.R. Morrison, Electrochemistry at Semiconductor and Oxidized Metal Electrodes, Plenum Press, New York, 1980.
[12] D. Elliott, D.L. Zellmer, H.A. Laitinen, J. Electrochem. Soc. 117 (1979) 1343.
[13] N.L. Wu, S.Y. Wangind, I.A. Rusakova, Science 285 (1999) 1375.
[14] N.L. Wu, in: Proceedings of the Sixth World Congress of Chemical Engineering, September 2001, Melbourne, Australia, pp. 23–27.
[15] Y. Wang, A. Suna, W. Mahier, R. Kasowski, J. Chem. Phys. 87 (1987) 7315.
[16] Y.S. He, J.C. Campbell, T.C. Murphy, J. Mater. Res. 8 (1993) 3131.